JACS
JOURNAL OF THE AMERICAN CHEMICAL SOCIETY

Communication

pubs.acs.org/JACS

# Reversible Visible-Light Tuning of Self-Organized Helical Superstructures Enabled by Unprecedented Light-Driven Axially Chiral Molecular Switches

Yan Wang,[†] Augustine Urbas,[‡] and Quan Li*[,†]

[†]Liquid Crystal Institute, Kent State University, Kent, Ohio 44242, United States

[‡]Materials and Manufacturing Directorate, Air Force Research Laboratory, WPAFB, Ohio 45433, United States

Supporting Information

**ABSTRACT:** Two enantiomeric light-driven azo molecular switches with axial chirality and extended conjugation were found to exhibit unprecedented reversible photoisomerization in both organic-solvent and liquid-crystal media only upon visible-light irradiation. When doped in an achiral liquid crystal with a different concentration, the chiral switch was able either to immediately induce an optically tunable helical superstructure or to retain an achiral liquid-crystal phase whose helical superstructure was induced and tuned reversibly upon visible-light irradiation. Furthermore, reversible dynamic red, green, and blue reflection achieved only by using visible light was demonstrated.

The ability to tune molecular self-organization with an external stimulus is a main driving force in the bottom-up nanofabrication of molecular devices. Light-driven chiral molecular switches or motors in liquid-crystal (LC) media capable of self-organizing into optically tunable helical superstructures undoubtedly represent such a striking example because of their unique property of selective reflection of light and its consequent potential applications.[1−4] Such systems can be achieved by doping chiral azobenzenes into an achiral nematic LC host to self-organize into an optically tunable helical superstructure (i.e., a chiral nematic phase). The resulting macroscopic helical superstructure can reflect light according to Bragg's law. The center wavelength $\lambda$ of the selective reflection is defined by $\lambda = np$, where $p$ is the pitch length of the helical structure and $n$ is the average index of refraction of the LC material. The ability of a chiral dopant to twist an achiral nematic LC phase [i.e., the helical twisting power (HTP, $\beta$)] is expressed in terms of the equation $\beta = (pc)^{-1}$ where $c$ is the chiral dopant concentration. The isomerization upon light irradiation can control the HTP and the reflection wavelength $\lambda$ of the helical superstructure, providing opportunities as well as challenges in fundamental science that would open the door for many applications such as tunable color filters,[5] tunable LC lasers,[6] and optically addressed displays that would require no drive electronics and could be made flexible.[7]

It is well-established that trans-to-cis isomerization of azobenzene is induced by UV light irradiation, whereas the reverse process, cis-to-trans isomerization, can occur thermally or photochemically with visible light.[8] Since the physical and chemical properties of the azobenzene configurational isomers are different, the reversible optically induced switching effect has been the basis for their applications. It is worth noting here that relying on UV light is undesirable in applications, since the use of UV light might result in material decomposition, strong absorption in the substrate (e.g., glass or plastic), poor penetration including through the substrate, etc. To the best of our knowledge, there have been no reports on chiral azo molecules that exhibit reversible visible-light-driven photoisomerization in both solvent and LC media.

Herein we report the synthesis of two novel enantiomeric light-driven azo molecular switches, (*S*,*S*)-**6** and (*R*,*R*)-**6**, that display axial chirality and have a larger conjugated system than azobenzene (Figure 1). To our surprise, they exhibited an unexpected reversible visible-light-driven photoisomerization in both organic-solvent and LC media (Figure 2). In other words, they exhibit fast, reversible trans-to-cis and cis-to-trans photoisomerization cycles, both induced only by using visible light. (*S*,*S*)-**6** and (*R*,*R*)-**6** exhibited high HTP values and considerable differences in HTP among their various states. Furthermore, their HTP in the initial state was found to increase upon visible-light irradiation, while the HTP of most chiral azobenzenes decreases upon UV-light irradiation.

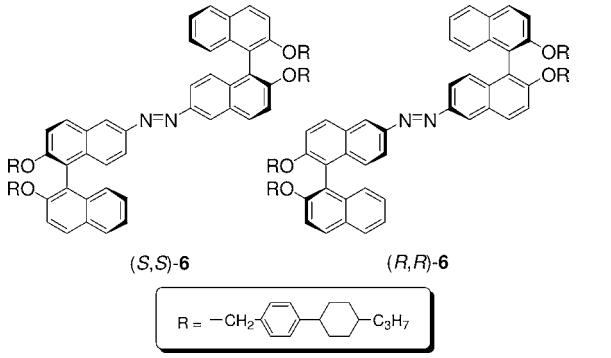


**Figure 1.** Chemical structures of light-driven axially chiral switches *trans*-(*S*,*S*)-**6** and *trans*-(*R*,*R*)-**6**.

**Received:** December 19, 2011
**Published:** February 7, 2012





dx.doi.org/10.1021/ja211837f | *J. Am. Chem. Soc.* 2012, 134, 3342−3345

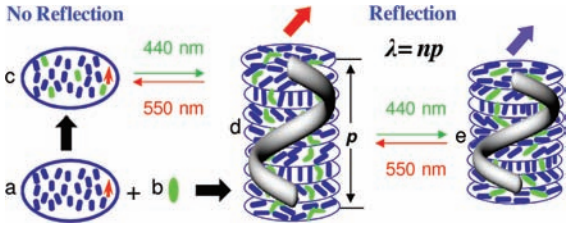


**Figure 2.** Schematic illustration of the mechanism for the reflection wavelength of light-driven chiral molecular switch (*S*,*S*)-**6** or (*R*,*R*)-**6** (green) in an achiral nematic LC medium (blue) reversibly tuned only by visible light: (a) achiral nematic host; (b) light-driven chiral switch or motor; (c) achiral photoresponsive nematic phase; (d, e) photoresponsive chiral nematic phase whose pitch length decreases in going from (d) to (e).

Reversible dynamic red, green, and blue reflection achieved only by using visible light was demonstrated.

Chiral switch (*S*,*S*)-**6** and its enantiomer were prepared by a facile synthesis. Their chemical structures were well-identified by $^{1}H$ and $^{13}C$ NMR spectroscopy, high-resolution mass spectrometry, and elemental analysis [see the Supporting Information (SI)]. Chiral switches (*S*,*S*)-**6** and (*R*,*R*)-**6** were chemically and thermally stable and exhibited the unexpected fast and reversible visible-light tunable behavior in both organic-solvent and LC media. For example, dark incubation of a solution of (*S*,*S*)-**6** in $CH_2Cl_2$ served to maximize the absorption at 407 nm corresponding to the initial state [i.e., *trans*-(*S*,*S*)-**6**]. Irradiation of this solution with visible light at 440 nm resulted in clean photoisomerization to a photostationary state (PSS), as evidenced by a decrease in the absorbance at 407 nm (Figure 3A). The $PSS_{440\ nm}$ for conversion of *trans*-(*S*,*S*)-**6** to *cis*-(*S*,*S*)-**6** was reached within ~40 s under visible-light irradiation at 440 nm, with ~45% of the trans isomer being tranformed to the cis isomer. The reverse process to give *trans*-(*S*,*S*)-**6** was reached within ~70 s under visible-light irradiation at 550 nm at room temperature (Figure 3B). Cycling from visible light at 440 nm for 45 s to visible light at 550 nm for 75 s was repeated many times without obvious fatigue (Figure S2 in the SI).

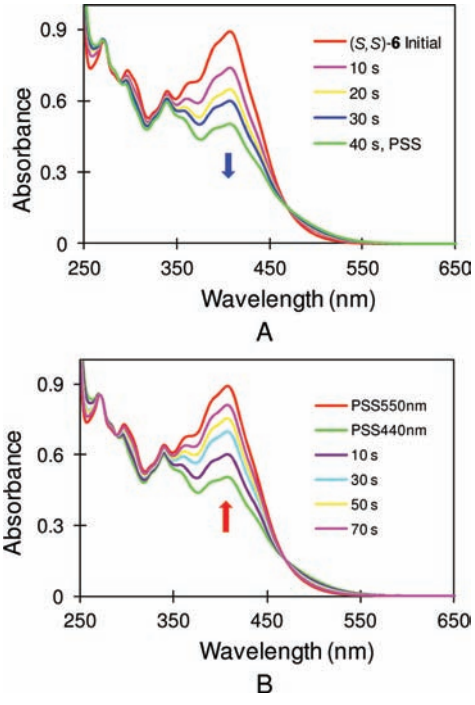


**Figure 3.** Changes in the UV–vis spectrum of (*S*,*S*)-**6** (17 μM in $CH_2Cl_2$) at room temperature in going (A) from the initial (trans) state to $PSS_{440\ nm}$ upon visible-light irradiation at 440 nm and (B) from $PSS_{440\ nm}$ to $PSS_{550\ nm}$ upon visible-light irradiation at 550 nm.

The effect of photoisomerization on the two chiral isomers was studied by circular dichroism (CD) spectroscopy. For example, the intense negative excitation of (*S*,*S*)-**6** at 210–240 nm, which is likely due to the long-axis-polarized transition of the naphthalene,[4d] reflects the absolute *S* configuration of the two binaphthyl moieties in the molecule. Figure 4 shows the change in the CD spectrum of (*S*,*S*)-**6** upon visible-light irradiation at 440 nm. (*R*,*R*)-**6** has the same property as (*S*,*S*)-**6** but with opposite handedness. The CD spectra of (*S*,*S*)-**6** and its enantiomer (*R*,*R*)-**6** exhibited an expected mirror image relationship with a strong sharp peak at ~230 nm (Figure S3).

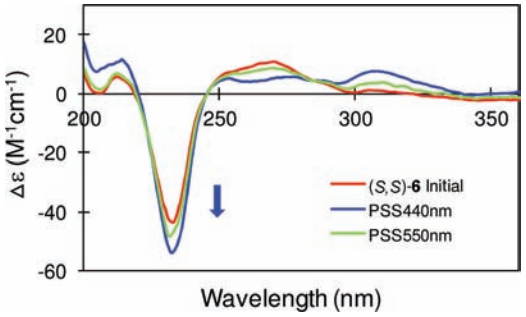


**Figure 4.** Changes in the CD spectrum of (*S*,*S*)-**6** (9.6 μM in $CH_3CN$) from the initial state (red) to $PSS_{440\ nm}$ upon visible-light irradiation at 440 nm (blue) and then back to $PSS_{550\ nm}$ upon visible-light irradiation at 550 nm (green).

The two chiral switches, doped in the commercially available achiral LC E7 with different concentration, were found to be able either to immediately induce chirality to form an optically tunable helical superstructure (i.e. a chiral nematic phase) or to retain an achiral LC phase whose chirality could be induced and tuned reversibly upon visible-light irradiation. For example, when 2.1 wt % chiral switch (*S*,*S*)-**6** was added to the achiral LC and capillary-filled into a 5 μm homeotropic cell, it induced an optically tunable helical superstructure, as evidenced by the characteristic fingerprint texture (Figure 5A), and the resulting helical superstructure could be reversibly and rapidly tuned using only visible light (Figure 5B,C). Its HTP was measured using the Grandjean–Cano method (Figures S5 and S6),[9] and

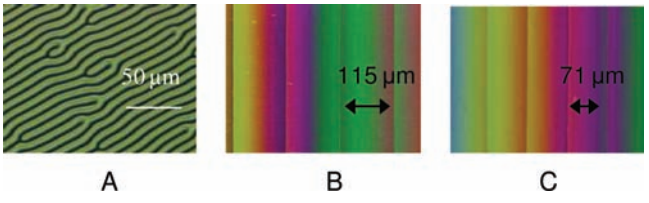


**Figure 5.** (A) Crossed-polarized texture of 2.1 wt % (*S*,*S*)-**6** in achiral nematic host E7 at room temperature in a 5 μm thick homeotropic aligned cell in its initial state. (B, C) Stripe-wedge Grandjean–Cano cell containing 2.1 wt% (*S*,*S*)-**6** in (B) the initial state and (C) after visible-light irradiation at 440 nm for 90 s.


dx.doi.org/10.1021/ja211837f | *J. Am. Chem. Soc.* 2012, 134, 3342–3345

found to be large, with considerable differences in HTP among various states (Table 1). (*S*,*S*)-**6** induced a left-handed helical

**Table 1. Helical Twisting Power $\beta$ (mol %, $\mu m^{-1}$) of (*S*,*S*)-6 and (*R*,*R*)-6 in Achiral Nematic LC E7 Initially and after Visible-Light Irradiation at 440 and 550 nm**

| dopant | initial | $PSS_{440\ nm}$ | $PSS_{550\ nm}$ |
|---|---|---|---|
| (*S*,*S*)-**6** | 52 | 89 | 58 |
| (*R*,*R*)-**6** | 52 | 89 | 58 |

superstructure, whereas its enantiomer (*R*,*R*)-**6** induced a right-handed helical superstructure. When the 2.1 wt % (*S*,*S*)-**6** sample was exposed to visible light at 440 nm, a decrease in pitch length was clearly observed as the change in the distance between the Cano lines, as shown in Figure 5B,C, whereas the pitch of the photoirradiated mixture increased or red-shifted with visible-light irradiation at 550 nm (Figure S5). Interestingly, when 1.5 wt % (*S*,*S*)-**6** was doped in achiral nematic E7, no chirality was induced (i.e., no helical superstructure was observed). The resulting phase was still an achiral nematic phase, as evidenced by the characteristic black texture in a homeotropic aligned cell (Figure 6A). This was

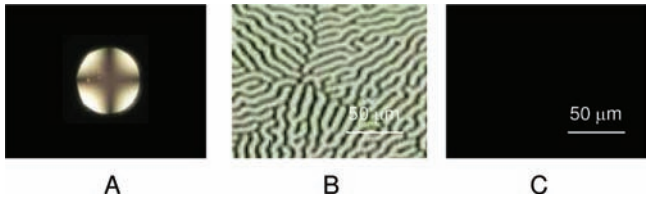


**Figure 6.** Crossed-polarized textures of 1.5 wt % (*S*,*S*)-**6** in achiral LC E7 at room temperature in a 5 $\mu$m thick homeotropic aligned cell. (A) initial state with conoscopic texture; (B) after visible-light irradiation at 440 nm for 30 s; (C) after subsequent visible-light irradiation at 550 nm for 15 s.

further confirmed by the inset conoscopic texture in Figure 6A. However, chirality (i.e., a helical superstructure) was induced in the achiral nematic phase upon visible-light irradiation at 440 nm, as evidenced by the characteristic fingerprint texture (Figure 6B). The reverse process (i.e., the disappearance of helical superstructure) occurred upon another visible-light irradiation at 550 nm. The reversible induction of helical superstructure resulted from the fact that the HTP in the cis state is higher than that in its trans state, which is less frequently observed in chiral azobenzenes. Typically, the HTP value decreases in going from the trans state to the cis state upon UV-light irradiation. The increase in HTP here might be attributed to a change in the dihedral angle of the binaphthyl groups.[3b,10]

The two chiral switches had a very large solubility in the achiral nematic LC host, which greatly facilitated doping to induce mesophase chirality and magnify the photocontrol effect. A mixture of 22.7 wt % (*S*,*S*)-**6** in LC E7 was capillary-filled into a 5 $\mu$m thick glass cell coated with a polyimide alignment layer for generating a planar alignment, and the cell was painted black on one side. Surprisingly, reversible and fast red, green, and blue (RGB) reflections were achieved in the cell. The RGB reflection colors with visible-light irradiation at 440 nm were achieved within ~30 s (Figure 7A). The reversible process across blue, green, and red reflection colors occurred upon visible-light irradiation at 550 nm or thermal relaxation in

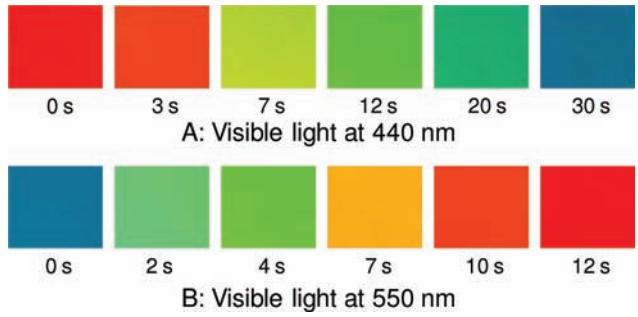


**Figure 7.** Reflection color images of 22.7 wt % (*S*,*S*)-**6** in LC E7 in a 5 $\mu$m thick planar cell taken from a polarized reflective mode microscope: (A) upon visible-light irradiation at 440 nm at different times; (B) reverse process upon visible-light irradiation at 550 nm at different times.

the dark. However, the light-driven reverse process was much faster than dark thermal relaxation. For instance, the photo-tuning of 22.7 wt % (*S*,*S*)-**6** in E7 across RGB occurred within 20 s using visible-light irradiation at 550 nm (Figure 7B), whereas its dark thermal relaxation across RGB took several hours. The reversible RGB phototuning process could be achieved in seconds with an increase in the light exposure intensity. With the commonly available LEDs and laser diodes at 440 and 550 nm, the prospect for realization of dynamic, light-directed reflection wavelength control is increasingly viable.

In conclusion, two novel enantiomeric light-driven chiral molecular azo switches with axial chirality and extended conjugation were synthesized. These exhibited an exceptional, reversible photoisomerization in both organic-solvent and LC media needing only visible-light irradiation. When doped in an achiral nematic LC with a larger concentration, the species was able to induce a helical superstructure that was tunable and dynamically reversible using only visible light. However, when doped in an achiral nematic LC with a lower concentration, it formed an optically tunable achiral nematic phase in which a helical superstructure could be induced reversibly upon visible-light irradiation. RGB reflection colors from a doped LC host were demonstrated by reversible visible-light-driven photo-isomerization. This new family of chiral azo dopants and the visible-light driven transitions provide an exciting impetus for the development of light-driven chiral molecular switches or motors with enhanced functionalities for practical device applications.

## ■ ASSOCIATED CONTENT

### Supporting Information

Materials and methods, synthetic procedures, measurement of pitch and HTP, and UV−vis and CD spectra. This material is available free of charge via the Internet at http://pubs.acs.org.

## ■ AUTHOR INFORMATION

### Corresponding Author

qli1@kent.edu

### Notes

The authors declare no competing financial interest.

## ■ ACKNOWLEDGMENTS

This work was supported by the Air Force Office of Scientific Research (AFOSR FA9950-09-1-0193 and FA9550-09-1-0254).

We thank R. S. Zola, Y. Li, L. Jin, X. Ma, and C. Xue for discussions and characterization assistance.

## REFERENCES

(1) (a) Eelkema, R.; Feringa, B. L. *Org. Biomol. Chem.* **2006**, *4*, 3729. (b) Pieraccini, S.; Masiero, S.; Ferrarini, A.; Spada, G. P. *Chem. Soc. Rev.* **2011**, *40*, 258. (c) Mallia, V. A.; Tamaoki, N. *Chem. Soc. Rev.* **2004**, *33*, 76.

(2) (a) Van Delden, R. A.; Koumura, N.; Harada, N.; Feringa, B. L. *Proc. Natl. Acad. Sci. U.S.A.* **2002**, *99*, 4945. (b) Eelkema, R.; Feringa, B. L. *Chem.— Asian J.* **2006**, *1*, 367. (c) Eelkema, R.; Pollard, M. M.; Vicario, J.; Katsonis, N.; Ramon, B. S.; Bastiaansen, C. W. M.; Broer, D. J.; Feringa, B. L. *Nature* **2006**, *440*, 163. (d) Eelkema, R.; Pollard, M. M.; Katsonis, N.; Vicario, J.; Broer, D. J.; Feringa, B. L. *J. Am. Chem. Soc.* **2006**, *128*, 14397.

(3) (a) Pieraccini, S.; Masiero, S.; Spada, G. P.; Gottarelli, G. *Chem. Commun.* **2003**, 598. (b) Pieraccini, P.; Gottarelli, G.; Labruto, R.; Masiero, S.; Pandolini, O.; Spada, G. P. *Chem.—Eur. J.* **2004**, *10*, 5632. (c) Mathews, M.; Tamaoki, N. *J. Am. Chem. Soc.* **2008**, *130*, 11409. (d) Yoshioka, T.; Ogata, T.; Nonaka, T.; Moritsugu, M.; Kim, S. N.; Kurihara, S. *Adv. Mater.* **2005**, *17*, 1226.

(4) (a) Li, Q.; Green, L.; Venkataraman, N.; Shiyanovskaya, I.; Khan, A.; Urbas, A.; Doane, J. W. *J. Am. Chem. Soc.* **2007**, *129*, 12908. (b) Green, L.; Li, Y.; White, T.; Urbas, A.; Bunning, T. J.; Li, Q. *Org. Biomol. Chem.* **2009**, *7*, 3930. (c) White, T. J.; Bricker, R. L.; Natarajan, L. V.; Tabiryan, N. V.; Green, L.; Li, Q.; Bunning, T. J. *Adv. Funct. Mater.* **2009**, *19*, 3483. (d) Mathews, M.; Zola, R. S.; Hurley, S.; Yang, D.-K.; White, T. J.; Bunning, T. J.; Li, Q. *J. Am. Chem. Soc.* **2010**, *132*, 18361. (e) Ma, J.; Li, Y.; White, T.; Urbas, A.; Li, Q. *Chem. Commun.* **2010**, *46*, 3463.

(5) (a) Ha, N. A.; Ohtsuka, Y.; Jeong, S. M.; Nishimura, S.; Suzaki, G.; Takanishi, Y.; Ishikawa, K.; Takezoe, H. *Nat. Mater.* **2008**, *7*, 43. (b) Mitov, M.; Dessaud, N. *Nat. Mater.* **2006**, *5*, 361.

(6) (a) Morris, S. M.; Hands, P. J. M.; Findeisen-Tandel, S.; Cole, R. H.; Wilkinson, T. D.; Coles, H. J. *Opt. Express* **2008**, *16*, 18827. (b) Furumi, S.; Tamaoki, N. *Adv. Mater.* **2010**, *22*, 886.

(7) (a) Montbach, E.; Venkataraman, N.; Khan, A.; Shiyanovskaya, I.; Schneider, T.; Doane, J. W.; Green, L.; Li, Q. *SID Int. Symp. Dig. Tech. Pap.* **2008**, 919. (b) Venkataraman, N.; Miagyar, G.; Montbach, E.; Khan, A.; Schneider, T.; Doane, J. W.; Green, L.; Li, Q. *J. Soc. Inf. Disp.* **2009**, *17*, 869. (c) Li, Q.; Li, Y.; Ma, J.; Yang, D.-K.; White, T. J.; Bunning, T. J. *Adv. Mater.* **2011**, *23*, 5069. (d) Li, Q.; Green, L.; Doane, J. W.; Asad, A.; Venkataraman, N.; Shiyanovskaya, I. U.S. Pat. Appl. Publication 0237906, 2007.

(8) (a) Ichimura, K. In *Photochromism: Molecules and Systems*; Dürr, H., Bouas-Laurent, H., Eds.; Elsevier: Amsterdam, 1990. (b) Tamai, N.; Miyasaka, H. *Chem. Rev.* **2000**, *100*, 1875.

(9) Dierking, I. *Textures of Liquid Crystals*; Wiley-VCH: Weinheim, Germany, 2003.

(10) (a) Gottarelli, G.; Spada, G. P.; Bartsch, R.; Solladié, G.; Zimmermann, R. *J. Org. Chem.* **1986**, *51*, 589. (b) Pieraccini, S.; Ferrarini, A.; Fuji, K.; Gottarelli, G.; Lena, S.; Tsubaki, K.; Spada, G. P. *Chem.—Eur. J.* **2006**, *12*, 1121.